Outer membrane changes enable evolutionary escape from bacterial predation

Subham Mridha[1,2,§,#], Sarah-Luise Loose[1,*], Ove Ch. Mattmann[1,2,*], Saskia Isele[1], Rolf Kümmerli[2] and Simona G. Huwiler[1,#]

[1]Department of Plant and Microbial Biology, University of Zurich, Zurich, Switzerland

[2]Department of Quantitative Biomedicine, University of Zurich, Zurich, Switzerland

*** These authors contributed equally to this work**

§ Current address: Department of Microbiology, Perelman School of Medicine, University of Pennsylvania, Philadelphia, United States of America

 # Correspondence:
Subham Mridha & Simona Huwiler
subhammridha@yahoo.com & simona.huwiler@uzh.ch

Abstract

To combat antimicrobial resistant pathogens, natural predatory bacteria, like *Bdellovibrio bacteriovorus*, represent potential alternatives. *B. bacteriovorus* could be particularly potent as it kills a broad range of human bacterial pathogens, however, it remains unclear whether prey can evolve genetically-determined resistance against predation. Here, we show that the model bacterium *Escherichia coli* K-12 consistently evolves resistance against *B. bacteriovorus* during experimental evolution. Selection for resistance scaled positively with predation pressure and was widespread after two cycles of predator exposure. Like antibiotics, predation resistance was costly, manifesting in a trade-off between predation resistance and fitness in the absence of predators. Genetic analysis identified changes in outer membrane porin OmpF as common resistance mechanism, while a mutation in cell envelope lipopolysaccharide-modifying enzyme WaaF was rarer but also conferred predation resistance. Our study uncovers evolutionary and mechanistic aspects of prey escape from predation, generating important knowledge on predator-prey interactions and to advance sustainable treatments.

Keywords: predator-prey interaction, predatory bacteria, *Escherichia coli*, *Bdellovibrio bacteriovorus*, predation resistance, evolution, prey escape

Introduction

Bacterial resistance to conventional antibiotics is a major public health concern, that led to 1.27 million deaths in 2019[1]. This urgently calls for the discovery of novel antibiotics and alternative treatment strategies[2–4]. One promising alternative involves the use of natural bacterial predators including bacteriophages (viruses of bacteria)[5] and predatory bacteria[3,6], which are environmentally widespread[7]. While phage therapy is currently extensively studied[2], much less is known about the potential of predatory bacteria, like *Bdellovibrio bacteriovorus*, that kill and invade pathogenic bacteria and are therefore considered 'living antibiotics'[3,6]. *B. bacteriovorus* is capable of killing growing and stationary phase bacterial prey cells, and in addition irrespective of their antibiotic resistance[8–10].

Similar to bacteriophages, *B. bacteriovorus* is neither toxic nor pathogenic to eukaryotic cells and is therefore of great promise[3,6]. However, key differences exist between the two predator types. For example, bacteriophages are typically very specific to prey strains, whereas *B. bacteriovorus* is a generalist with a broad prey range[11,12]. This makes *B. bacteriovorus* suitable to treat polymicrobial infections[11,13]. Moreover, there seem to be few defence and immunity mechanisms present among prey species to defend themselves against *B. bacteriovorus*[14,15]. This contrasts with the over hundred specific bacterial defence and immune systems reported against bacteriophages[16]. Thus, *B. bacteriovorus* might be a more effective treatment under certain circumstances, compared to traditional antibiotics and bacteriophages.

Despite these promising aspects, little is known on the selection pressures that *B. bacteriovorus* may impose on its prey and the evolutionary responses it may trigger[17–19]. Some evolutionary studies, focussing on predator-prey interactions, reported evidence for resistance evolution[17–19] but did not explore the underlying mechanisms on a phenotypic and genotypic level. While recognition of the prey and prey invasion is likely multifactorial[20,21], potentially hindering fast resistance formation, prey resistance has been described transient[3,22]. One study described a form of phenotypic (plastic) resistance, whereby several prey species developed a transient yet reversible stage of predation resilience[22]. Finally, several studies highlighted that secretion systems[23] and secreted compounds such as quorum-sensing signals[24,25], indole[26] and cyanide[27] may offer some protection from *B. bacterivorous* predation, while the presence of paracrystalline protein surface (S-) layers seems to prevent killing in certain bacterial species[14].

50 To obtain a systematic and in-depth understanding of the potential of prey to evolve resistance to
51 *B. bacteriovorus*, we performed an experimental prey evolution study with the model organism *E. coli*
52 K-12 as prey and *B. bacteriovorus* HD100 as predator. Upon repeated and intermittent exposure of
53 prey to different predator concentrations, we found strong evidence that *E. coli* K-12 predominantly
54 evolves genetically-based predation resistance under high predatory pressure, whereas increased
55 growth due to media adaptation and phenotypic effects played minor roles. Evolutionary escape from
56 predation evolved repeatedly across independently evolved prey lineages. Predation resistance is costly
57 and manifested in a negative association between the resistance level of a lineage and its growth in the
58 absence of predation. A combination of population sequencing with high genome coverage and single-
59 gene deletion mutant experiments revealed that mutations in the outer membrane porin OmpF, and an
60 enzyme (WaaF) involved in lipopolysaccharide (LPS) modification are involved with resistant
61 phenotypes. These results suggest that the prey modifies different potential points of contact with the
62 predator[15,20]. Our study elucidates the ecological context, the evolutionary path, and the molecular
63 mechanisms of prey resistance evolution against *B. bacteriovorus*, generating key knowledge for the
64 development of bacterial predators as sustainable 'living antibiotics'.

65

66 # Results

67 **Experimental evolution leads to increased prey growth**

68 We experimentally evolved *E. coli* K-12 prey under no, low and high predatory pressures of
69 *B. bacteriovorus* HD100 in eightfold replication. Experimental prey evolution was conducted for 15
70 alternate cycles of predation and prey recovery (Fig. 1a, Extended Data Fig. 1). After prey evolution,
71 we subjected all evolved prey lineages to the predation pressure they experienced during experimental
72 evolution. We found significant growth differences across the three predatory pressures (ANOVA:
73 $F_{2,141} = 8780.2$, $p < 0.0001$). All *E. coli* lineages evolved without predator grew significantly better
74 than the ancestor (red dotted line), which indicates media adaptation (Fig. 1b+e). For prey lineages
75 evolved with predators, we observed that five low-predator evolved lineages (L1-L5, Fig. 1c+f) and
76 all high-predator evolved lineages (H1-H8, Fig. 1d+g) showed significant growth recovery relative to
77 the ancestor subjected to predation (black dotted line). For most of these lineages (84.6%), growth
78 recovery was partial, while only two lineages (H4, H5, 15.4%) showed complete recovery, compared
79 to the unchallenged ancestor. Moreover, growth under predation was higher for prey lineages evolved

80 under high than under low predatory pressure. Altogether, these results suggest that prey evolved
81 partial resistance to predation and that higher predation pressure selected for higher levels of resistance.

82

83 **Predation and not media adaptation drives resistance evolution**

84 Media adaptation could be a simple explanation for the observed resistance phenotypes because faster
85 growth would allow the prey to outpace the predator's killing speed. If this hypothesis holds true we
86 expect that no-predator evolved lineages, which showed highly improved growth, should be able to
87 resist predation. We found no support for this hypothesis as all no-predator evolved lineages were still
88 fully susceptible to predation (Fig. 2a, c). Instead, our results show that lineages L1-L5 (which evolved
89 partial resistance under low predation) were also able to grow under high predatory pressure (Fig. 2b,
90 d). We even observed slightly increased growth in a previously unnoticed lineage (L8). Together, these
91 results indicate that adaptations are predation-specific and not driven by media adaptation.

92

93 **Predation resistance arises early and remains persistent over time**

94 Next, we examined the temporal pattern of predation resistance evolution. We noticed that prey optical
95 density (OD_{600nm}) already increased at the second evolution cycle and fluctuated at a relatively high
96 level thereafter (Extended Data Fig. 1a). To verify that resistance arose early, we repeated the growth
97 experiments shown in Fig. 1b-g with all high-predator lineages (H1-H8) from the 2nd and 5th evolution
98 cycle (Extended Data Fig. 1 and 2). These analyses confirmed that predation-resistant phenotypes
99 emerged early on during experimental evolution as all lineages could readily grow under high predation
100 pressure at evolution cycle 2, with barely any growth differences existing compared to later evolution
101 cycles 5 and 15 (Extended Data Fig. 1 and 2). Hence, predation resistance evolved early and once
102 emerged within a prey lineage it remained persistent over generations.

103

104 **Trade-off between predation resistance and prey growth in the absence of predation**

105 Antibiotics resistance is often associated with fitness costs in the absence of antibiotics[28,29]. Here, we
106 tested whether a similar trade-off occurs for *E. coli* in the context of predation resistance. To investigate

107 this, we grew all evolved lineages without predators and calculated their growth rate relative to the
108 ancestor. Relative growth rates differed significantly across predatory pressures (ANOVA: $F_{2,141}$ =
109 460.42, $p < 0.0001$), and were highest in no-predator evolved *E. coli* lineages (Fig. 3a, d), followed by
110 low-predator evolved lineages with growth rates similar to the ancestor (Fig. 3b, e) and high-predator
111 evolved lineages with generally lower growth rate than the ancestor (Fig. 3c, f). When contrasting these
112 growth rates against relative prey resistance (quantified as relative growth integral under high predatory
113 pressure), we found a significant negative correlation between predation resistance and prey fitness,
114 indicating the predicted trade-off (Fig. 3g). Thus, our findings corroborate that *E. coli* resistance
115 mechanisms are costly in the absence of *B. bacteriovorus* predation.

116

117 **High consistency in resistance levels among single clones**

118 Based on the detected trade-off between predation resistance and population prey growth, we wondered
119 whether there is heterogeneity in predation resistance among clones within prey populations.
120 Consequently, we analysed the predation resistance profile of six randomly isolated clones from each
121 of the eight high-predator lineages (15th cycle, 48 clones) and found that all clones showed consistently
122 high predation resistance. This shows that clones did not separate into susceptible and resistant
123 phenotypes (Extended Data Fig. 4 and 5) and thus did not segregate along a trade-off line within
124 populations. This result further indicates that the mechanisms conferring resistance to predation likely
125 operate at the individual and not at the group level of the prey. Such group-level mechanisms were
126 proposed to operate via the secretion of small soluble substances (quorum-sensing signals, indole,
127 cyanide)[24–27] and are expected to protect not only the evolved producers but also susceptible wildtype
128 cells.

129

130 **Mutation frequency in the prey genome peaks under high predatory pressure**

131 To uncover the genetic basis of putative resistance mechanisms, we sequenced all 24 evolved *E. coli*
132 lineages (N1-8: no predation, L1-8: low predation, H1-8: high predation) after the 15th evolution cycle
133 along with the original ancestor with high sequencing depth. The Illumina sequencing reads were
134 mapped to the reference genome of *E. coli* K-12 MG1655 and multi-sample variant calling with a
135 frequency cutoff of 5% was performed. We focused on *E. coli* genes that had mutations in evolved

136 lineages but not in the ancestor (Extended Data Fig. 6). We excluded mutated rRNA and transposase
137 genes because they did not correlate with any of the three evolution conditions (Extended Data Fig. 7).
138 Using these filters, we uncovered 43 mutated genes of which 17 occurred in N-lineages, 17 in L-
139 lineages and 30 in H-lineages (Fig. 4a). A total of 26 genes mutated exclusively under predatory
140 pressure (Fig. 4a), and thus reflect the top candidates potentially explaining resistance phenotypes. H-
141 lineages, had more exclusive gene mutations than L-lineages (18 vs. 5, Fig. 4b). Moreover, there were
142 fewer high-frequency mutations (>70%) among L-lineages than among H-lineages (Fig. 4b), which is
143 likely explained by the higher selection pressure.

144

145 **Outer membrane porin OmpF mutations repeatedly arose and confer resistance to predation**

146 Next, we conducted a cluster analysis (Fig. 4b) and analyzed the functions of the mutated gene products
147 including mutation types and (predicted) amino acid changes (Fig. 4c, Extended Data Table 1). These
148 analyses yielded *ompF*, encoding the outer membrane porin F, as the most frequently mutated gene.
149 Four H-lineages (H2, H4, H6 & H7) and two L-lineages (L1, L2) had mutations in this gene. Moreover,
150 lineage H3 had a point mutation in the upstream region of *ompF* (Extended Data Fig. 8) and lineage
151 H8 had an inframe insertion in *envZ* (Extended Data Table 1), which encodes a sensor histidine kinase
152 involved in OmpF regulation[30]. Mutation frequencies were high (73.6%-100%) in all lineages except
153 in L2. The sequencing of six individual clones per H-lineage showed that mutations in *ompF* and *envZ*
154 were present in all clones (Extended Data Fig. 9). Overall, there were no major differences in
155 mutational patterns between clonal and population level sequencing (Extended Data Fig. 9), reinforcing
156 the view of selective sweeps of a few beneficial mutations through populations. Mutation types in
157 *ompF* include missense variants (H2), frameshifts (H4, H6, H7) and direct stop gains (L1, L2) (Fig.
158 4b, c, Extended Data Fig. 8, Extended Data Table 1), indicating that most observed mutations probably
159 lead to OmpF function loss.

160 To directly test whether the loss of OmpF (a known attachment side for phages and known to be critical
161 for effective *B. bacteriovorus* predation[15]) confers resistance to predation, we generated a clean, single
162 deletion Δ*ompF* mutant based on the *E. coli* KEIO library (details in methods, Supplementary Online
163 material Table SOnline1). First, we confirmed that *E. coli* KEIO reference strain (BW25113) was fully
164 susceptible to *B. bacteriovorus* and grew well in the absence of predation (Fig. 5a,b), thus showing
165 similar responses as the *E. coli* K-12 ancestor (Fig. 1b,d and 2a,b). We then subjected the Δ*ompF*

166 mutant to no and high predation pressures and tracked its growth. We found this mutant to be
167 completely resistant to predation, showing full growth recovery under high predator exposure (Fig.
168 5a,b). We repeated the above experiments with a Δ*envZ* clean deletion mutant and found that this
169 mutant was still susceptible to predation, in agreement with Mun et al.[15] (Fig. 5a, b). This is
170 unsurprising because the experimentally evolved *envZ* mutant involved an inframe insertion [insertion
171 of Lys-Thr-Trp-Leu between Leu135 and Lys136] and not a deletion. We suspect that the insertional
172 mutation in our experiment might upregulate OmpR, resulting in lower levels of OmpF. We thus
173 conclude that functional changes in EnvZ, but not loss-of-function, could confer predation resistance.
174 In summary, our results indicate that predation resistance is primarily driven by OmpF loss-of-function
175 mutations.

176

177 **Mutations in *truA* cause costly prey morphology change**

178 In lineage H8, a high frequency mutation occurred in *truA* (100%, missense: Val200Ala) in addition
179 to the above-described *envZ* mutation (77.5%). The *truA* gene encodes the tRNA pseudouridine
180 synthase A important for protein synthesis[31]. Phase-contrast microscopy revealed that cells from
181 lineage H8 no longer separated properly after cell division resulting in cells being thinner and longer
182 (Extended Data Fig. 3a-c). Experiments with a Δ*truA* clean deletion mutant confirmed division
183 abnormalities (Extended Data Fig. 3), matching previously reported results on the effect of *truA*
184 disruption[32]. No such abnormalities in cell morphology occurred in the other H- and L-lineages
185 (Extended Data Fig. 3, Fig. SOnline1). However, deletion of *truA* did not result in predation resistance
186 but was rather associated with severe fitness costs in the absence of predation (Fig. 5). We hypothesise
187 that the resistance phenotype observed in the evolved *truA* mutant is masked in the clean deletion
188 mutant due the detrimental effects on cell division (Fig. 5). Further, our mutation frequency data
189 suggest that the missense mutation in *truA* (100%) happened first and was associated with a drop in
190 final OD_{600nm} after the recovery phase of early evolution cycles 1-5. Growth only recovered in later
191 cycles, likely due to the additional mutation in *envZ* (77.5%), probably partly compensating the fitness
192 drop (Extended Data Fig. 1b). Altogether, our results indicate that resistance to predation may occur
193 through cell morphology changes. However, such events might be rare due to the severe fitness costs
194 typically associated with changes in fundamental cell physiological processes.

195

196 **Mutation in LPS synthesis gene *waaF* confers partial resistance to predation**

197 In lineage H5, a high frequency mutation occurred in *waaF* (100%, missense: Ala255Glu), encoding
198 an heptosyltransferase involved in the biosynthesis of the lipopolysaccharide (LPS) inner core[33]. We
199 hypothesized that modification or abolishment of outer membrane structures could represent a
200 mechanism through which *E coli* can become resistant to predation. In support of our hypothesis, we
201 found that a Δ*waaF* clean deletion mutant showed partial and significant resistance to predation (Fig.
202 5a,b). The same hypothesis could also hold true for the high frequency mutation observed in *waaB*
203 (lineage H4, 87.5%, stop codon gained) encoding a galactosyltransferase involved in LPS biosynthesis.
204 However, contrary to our expectation we did not find Δ*waaB* (clean deletion mutation) to be resistant
205 to predation (Fig. 5a,b). Instead, it showed significant growth improvements in the absence of predation
206 (Fig. 5c,d). Because the mutation in *waaB* occurred together with an *ompF* mutation in lineage H4 we
207 conclude that WaaB loss-of-function does not confer predation resistance but is beneficial in an already
208 resistant lineage, showing the highest growth recovery under predation among all H-lineages (Fig. 1g).

209

210 # Discussion

211 Historical records on antibiotics tell us that bacterial pathogens have evolved resistance to every single
212 drug used in clinics. Nowadays, it is therefore imperative to understand putative mechanisms and paths
213 to resistance already during the development of new antibacterials[34,35]. In our study, we performed this
214 task for the predatory bacterium *B. bacteriovorus*, which is regarded as a potential 'living antibiotic'
215 preying on human pathogens. We found that the model prey *E. coli* K-12 MG1655 consistently evolved
216 resistance against predation through two main mechanisms: change in the outer membrane porin OmpF
217 (several independent events), and change in WaaF (one event), an enzyme involved in outer membrane
218 LPS biosynthesis. These mechanisms suggest that selection acts on cell-membrane associated traits
219 that form the first line of contact between prey and predators. The uncovered resistance mechanisms
220 are similar to the ones observed to evolve against bacteriophages[36,37] (loss/alteration of host
221 receptors[38,39]) and against membrane-targeting polymyxin antibiotics (LPS modifications)[40].

222 OmpF enables *E. coli* to import and export small molecules via passive diffusion. Osmolarity of the
223 environment likely effects prey susceptibility towards *B. bacteriovous*. It is known that *E. coli*
224 expresses high levels of OmpF under neutral pH, whereas high osmolarity leads to its
225 downregulation[41]. OmpF serves as an entry point for bacterial toxins (colicin) and antibiotics[42–44] while

226 simultaneously serving as docking site for certain bacteriophages[38,39]. However, its role in the
227 interaction with *B. bacteriovorus* is not yet resolved, apart from the fact that the deletion of OmpF
228 slows predation rate[15] and that mutations in this gene are under selection in response to predation in
229 our study. We can thus only speculate about how loss or impairment of OmpF could foster predation
230 resistance, and we propose three scenarios. Firstly, change of OmpF could prevent predators to use the
231 porin as a docking site for attachment[15], similar to phage invasion[38,39]. Secondly, OmpF might serve as
232 an 'overpressure valve' equilibrating the osmotic pressure building up when *B. bacteriovorus* enters
233 the prey periplasm. Loss of OmpF or a reduction in its small molecule transport rate might compromise
234 this function and presumably slow down predator entry. Thirdly, loss of OmpF could reduce the entry
235 of potential, hypothetical small molecules secreted by the predator. Such molecules could manipulate
236 the prey during attachment and recent evidence indicates that *B. bacteriovorus* can kill the prey even
237 without subsequent entry[45]. Altogether, our results combined with previous reports indicate that OmpF
238 is a mutational hotspot in the context of resistance evolution against antibiotics, bacteriophages, and
239 predatory *B. bacteriovorus*.

240 Important to note is that the relevance of OmpF for successful *B. bacteriovorus* predation seems to
241 depend on the prey species[15]. For example, deletion of OmpF in *Salmonella enterica* did not reduce
242 prey killing[15]. Instead, it was reported that the LPS core has a major influence on attachment[46,47]. This
243 finding combined with our results (showing that mutations in LPS-modifying enzymes WaaF and
244 WaaB were under selection) strongly support the view that LPS structure takes on an important role in
245 the interactions with predators. Work with bacteriophages revealed two opposite roles for LPS
246 (particularly the long O-antigens): depending on their specific structure they may act as primary
247 receptors for attachment or block attachment to the outer membrane[38,39]. Several lines of evidence
248 suggest that the dual role also applies to interactions with *B. bacteriovorus*[20,46,48]. First, a phage-tail
249 fiber protein homolog of *B. bacteriovorus* was indeed shown to bind to multiple bacterial surface
250 glycans/LPS in multiple prey species (*E. coli* K-235, *Serratia marcescens* and *Proteus mirabilis*)[20].
251 Second, attachment to prey is slowed down when predators are confronted with complex O-antigens
252 as opposed to shorter LPS only featuring the core oligosaccharides in several species (*S. enterica*,
253 *E. coli*, *Vibrio cholerae*)[46 48]. In sum, our results indicate that evolutionary change in LPS structure can
254 modulate prey-predator interactions as observed for bacteriophage-bacteria interactions.

255 At first sight, our results on repeated resistance evolution seem to dampen the hope for predatory
256 bacteria to become sustainable antibacterial treatments. Nonetheless, our experiments also revealed

257 good news. Particularly, the strong fitness trade-off between resistance to predation and growth in the
258 absence of predation highlights that genetically manifested predation resistance is costly,
259 compromising cellular functionality. This phenomenon could limit the spread of resistant prey as they
260 are weak competitors and probably cleared away more efficiently by macrophages. There are concepts
261 to leverage such competitive constraints to increase treatment sustainability[28,49]. A key condition for
262 leveraging on competitive constraints is that the pathogen is eliminated before compensatory mutations
263 arise. We observed two putative compensatory mutations in our experiments (mutation in *waaB* in the
264 background of an *ompF* mutant; mutation in *envZ* in the background of a *truA* mutant). Clearly, more
265 research is required to understand the propensity of resistant prey mutants (with and without
266 compensatory mutations) to spread. Moreover, it will be important to test whether similar evolutionary
267 patterns (type of mutants, compensatory mutants and speed of resistance development) are detected
268 when using predatory *B. bacteriovorus* against pathogenic bacteria and clinical isolates as prey to
269 assess the sustainability of this 'living antibiotic'.

270 To conclude, we like to emphasize two important points regarding prey resistance against bacterial
271 predation by *B. bacteriovorus*. First, resistance mechanisms do not need to offer complete protection
272 to escape predation. Instead, it suffices to alter the balance between prey growth and killing rate. In our
273 experiment, we detected a decrease in killing rate (by mutations in *ompF* and *waaF*), but no increase
274 in prey growth rate. Second, while we focused on predation resistance through mutation and selection
275 processes, previous work has reported 'plastic' resistance phenotypes, occurring after short timescale
276 exposures, offering transiently protection against *B. bacteriovorus*[22]. Such plastic effects also surface
277 in response to colistin exposure (i.e. change in membrane polarity) and might well have occurred in
278 our experiments (e.g., in resistant prey lineages exposed to low predatory pressure with few low
279 frequency genetic mutations). A key task for future studies is to integrate all these aspects and to
280 understand the dynamics of prey resistance and predation escape under situations that are closer to
281 clinical settings – for example using clinical pathogen isolates, assessing treatment efficacy in spatially
282 structured human cell cultures, and allowing predators to co-evolve with the prey. Only with such
283 integrative knowledge, we can ensure the long-term sustainability of *B. bacteriovorus* as a 'living
284 antibiotic', efficient in targeting multi-drug resistant pathogens, in clinically relevant contexts.

285

286 # References (Main text)

287 1. Murray, C. J., et al. Global burden of bacterial antimicrobial resistance in 2019: a systematic
288 analysis. *The Lancet* **399,** 629–655 (2022).

289 2. Pirnay, J.-P., et al. Personalized bacteriophage therapy outcomes for 100 consecutive cases: a
290 multicentre, multinational, retrospective observational study. *Nat Microbiol* **9,** 1434–1453
291 (2024).

292 3. Sockett, R. E. & Lambert, C. Bdellovibrio as therapeutic agents: a predatory renaissance? *Nat*
293 *Rev Microbiol* **2,** 669–675 (2004).

294 4. Konwar, A. N., Hazarika, S. N., Bharadwaj, P. & Thakur, D. Emerging Non-Traditional
295 Approaches to Combat Antibiotic Resistance. *Curr Microbiol* **79,** 330 (2022).

296 5. Koskella, B., Hernandez, C. A. & Wheatley, R. M. Understanding the Impacts of
297 Bacteriophage Viruses: From Laboratory Evolution to Natural Ecosystems. *Annu. Rev. Virol.* **9,**
298 57–78 (2022).

299 6. Atterbury, R. J. & Tyson, J. Predatory bacteria as living antibiotics - where are we now?
300 *Microbiology (Reading)* **167,** (2021).

301 7. Lai, T. F., Ford, R. M. & Huwiler, S. G. Advances in cellular and molecular predatory biology
302 of *Bdellovibrio bacteriovorus* six decades after discovery. *Front. Microbiol.* **14,** 1168709
303 (2023).

304 8. Saralegui, C., Herencias, C., Halperin, A. V., De Dios-Caballero, J., Pérez-Viso, B., Salgado,
305 S., Lanza, V. F., Cantón, R., Baquero, F., Prieto, M. A. & Del Campo, R. Strain-specific
306 predation of *Bdellovibrio bacteriovorus* on *Pseudomonas aeruginosa* with a higher range for
307 cystic fibrosis than for bacteremia isolates. *Sci Rep* **12,** 10523 (2022).

308 9. Upatissa, S., Mun, W. & Mitchell, R. J. Pairing Colicins B and E5 with *Bdellovibrio*
309 *bacteriovorus* To Eradicate Carbapenem- and Colistin-Resistant Strains of *Escherichia coli*.
310 *Microbiol Spectr* **11,** e00173-23 (2023).

311 10. Sun, Y., Ye, J., Hou, Y., Chen, H., Cao, J. & Zhou, T. Predation Efficacy of *Bdellovibrio*
312 *bacteriovorus* on Multidrug-Resistant Clinical Pathogens and Their Corresponding Biofilms.
313 *Jpn J Infect Dis* **70,** 485–489 (2017).

314 11. Dashiff, A., Junka, R. A., Libera, M. & Kadouri, D. E. Predation of human pathogens by the
315 predatory bacteria *Micavibrio aeruginosavorus* and *Bdellovibrio bacteriovorus*: Predation by
316 *M. aeruginosavorus* and *B. bacteriovorus*. *Journal of Applied Microbiology* **110,** 431–444
317 (2011).

318 12. Jurkevitch, E., Minz, D., Ramati, B. & Barel, G. Prey Range Characterization, Ribotyping, and
319 Diversity of Soil and Rhizosphere *Bdellovibrio* spp. Isolated on Phytopathogenic Bacteria. *Appl*
320 *Environ Microbiol* **66,** 2365–2371 (2000).

321 13. Im, H., Choi, S. Y., Son, S. & Mitchell, R. J. Combined Application of Bacterial Predation and
322 Violacein to Kill Polymicrobial Pathogenic Communities. *Sci Rep* **7,** 14415 (2017).

323 14. Koval, S. F. & Hynes, S. H. Effect of paracrystalline protein surface layers on predation by
324 *Bdellovibrio bacteriovorus*. *J Bacteriol* **173,** 2244–2249 (1991).

325 15. Mun, W., Upatissa, S., Lim, S., Dwidar, M. & Mitchell, R. J. Outer Membrane Porin F in *E.*
326 *coli* Is Critical for Effective Predation by *Bdellovibrio*. *Microbiol Spectr* **10,** e03094-22 (2022).

327 16. Georjon, H. & Bernheim, A. The highly diverse antiphage defence systems of bacteria. *Nat Rev*
328 *Microbiol* **21,** 686–700 (2023).

329 17. Varon, M. Selection of predation-resistant bacteria in continuous culture. *Nature* **277,** 386–388
330 (1979).

331 18. Gallet, R., Alizon, S., Comte, P.-A., Gutierrez, A., Depaulis, F., van Baalen, M., Michel, E. &
332 Muller-Graf, C. D. M. Predation and Disturbance Interact to Shape Prey Species Diversity.
333 **170,** 143–154 (2007).

334 19. Gallet, R., Tully, T. & Evans, M. E. K. Ecological conditions affect evolutionary trajecory in a
335 predator-prey system. *Evolution* **63,** 641–651 (2009).

336 20. Caulton, S. G., Lambert, C., Tyson, J., Radford, P., Al-Bayati, A., Greenwood, S., Banks, E. J.,
337 Clark, C., Till, R., Pires, E., Sockett, R. E. & Lovering, A. L. *Bdellovibrio bacteriovorus* uses

338 chimeric fibre proteins to recognize and invade a broad range of bacterial hosts. *Nat Microbiol*
339 **9,** 214–227 (2024).

340 21. Chanyi, R. M., Ward, C., Pechey, A. & Koval, S. F. To invade or not to invade: two
341 approaches to a prokaryotic predatory life cycle. *Can J Microbiol* **59,** 273–279 (2013).

342 22. Shemesh, Y. & Jurkevitch, E. Plastic phenotypic resistance to predation by *Bdellovibrio* and
343 like organisms in bacterial prey. *Environmental Microbiology* **6,** 12–18 (2004).

344 23. Aharon, E., Mookherjee, A., Pérez-Montaño, F., Mateus Da Silva, G., Sathyamoorthy, R.,
345 Burdman, S. & Jurkevitch, E. Secretion systems play a critical role in resistance to predation by
346 *Bdellovibrio bacteriovorus*. *Research in Microbiology* **172,** 103878 (2021).

347 24. Hoshiko, Y., Nishiyama, Y., Moriya, T., Kadokami, K., López-Jácome, L. E., Hirano, R.,
348 García-Contreras, R. & Maeda, T. Quinolone Signals Related to Pseudomonas Quinolone
349 Signal-Quorum Sensing Inhibits the Predatory Activity of *Bdellovibrio bacteriovorus*. *Front.*
350 *Microbiol.* **12,** 722579 (2021).

351 25. Dwidar, M., Jang, H., Sangwan, N., Mun, W., Im, H., Yoon, S., Choi, S., Nam, D. & Mitchell,
352 R. J. Diffusible Signaling Factor, a Quorum-Sensing Molecule, Interferes with and Is Toxic
353 Towards *Bdellovibrio bacteriovorus* 109J. *Microb Ecol* **81,** 347–356 (2021).

354 26. Dwidar, M., Nam, D. & Mitchell, R. J. Indole negatively impacts predation by *B dellovibrio*
355 *bacteriovorus* and its release from the bdelloplast. *Environmental Microbiology* **17,** 1009–1022
356 (2015).

357 27. Mun, W., Kwon, H., Im, H., Choi, S. Y., Monnappa, A. K. & Mitchell, R. J. Cyanide
358 Production by *Chromobacterium piscinae* Shields It from *Bdellovibrio bacteriovorus* HD100
359 Predation. *mBio* **8,** e01370-17 (2017).

360 28. Andersson, D. I. & Hughes, D. Antibiotic resistance and its cost: is it possible to reverse
361 resistance? *Nat Rev Microbiol* **8,** 260–271 (2010).

362 29. Andersson, D. I. The biological cost of mutational antibiotic resistance: any practical
363 conclusions? *Current Opinion in Microbiology* **9,** 461–465 (2006).

364 30. Cai, S. J. & Inouye, M. EnvZ-OmpR Interaction and Osmoregulation in *Escherichia coli.*
365 *Journal of Biological Chemistry* **277,** 24155–24161 (2002).

366 31. Davis, D. R. & Poulter, C. D. Proton-nitrogen-15 NMR studies of *Escherichia coli* tRNAPhe
367 from HisT mutants: a structural role for pseudouridine. *Biochemistry* **30,** 4223–4231 (1991).

368 32. Tsui, H. C., Arps, P. J., Connolly, D. M. & Winkler, M. E. Absence of hisT-mediated tRNA
369 pseudouridylation results in a uracil requirement that interferes with *Escherichia coli* K-12 cell
370 division. *J Bacteriol* **173,** 7395–7400 (1991).

371 33. Gronow, S., Brabetz, W. & Brade, H. Comparative functional characterization *in vitro* of
372 heptosyltransferase I (WaaC) and II (WaaF) from *Escherichia coli*. *European Journal of*
373 *Biochemistry* **267,** 6602–6611 (2000).

374 34. Aminov, R. I. A Brief History of the Antibiotic Era: Lessons Learned and Challenges for the
375 Future. *Front. Microbio.* **1,** (2010).

376 35. Davies, J. & Davies, D. Origins and Evolution of Antibiotic Resistance. *Microbiol Mol Biol*
377 *Rev* **74,** 417–433 (2010).

378 36. Fang, Q., Feng, Y., McNally, A. & Zong, Z. Characterization of phage resistance and phages
379 capable of intestinal decolonization of carbapenem-resistant *Klebsiella pneumoniae* in mice.
380 *Commun Biol* **5,** 48 (2022).

381 37. Oechslin, F. Resistance Development to Bacteriophages Occurring during Bacteriophage
382 Therapy. *Viruses* **10,** 351 (2018).

383 38. Maffei, E., Shaidullina, A., Burkolter, M., Heyer, Y., Estermann, F., Druelle, V., Sauer, P.,
384 Willi, L., Michaelis, S., Hilbi, H., Thaler, D. S. & Harms, A. Systematic exploration of
385 *Escherichia coli* phage–host interactions with the BASEL phage collection. *PLoS Biol* **19,**
386 e3001424 (2021).

387 39. Nobrega, F. L., Vlot, M., De Jonge, P. A., Dreesens, L. L., Beaumont, H. J. E., Lavigne, R.,
388 Dutilh, B. E. & Brouns, S. J. J. Targeting mechanisms of tailed bacteriophages. *Nat Rev*
389 *Microbiol* **16,** 760–773 (2018).

390 40. Jochumsen, N., Marvig, R. L., Damkiær, S., Jensen, R. L., Paulander, W., Molin, S., Jelsbak, L.
391 & Folkesson, A. The evolution of antimicrobial peptide resistance in *Pseudomonas aeruginosa*
392 is shaped by strong epistatic interactions. *Nat Commun* **7,** 13002 (2016).

393 41. Kenney, L. J. & Anand, G. S. EnvZ/OmpR Two-Component Signaling: An Archetype System
394 That Can Function Noncanonically. *EcoSal Plus* **9,** 10.1128/ecosalplus.ESP-0001–2019 (2020).

395 42. Thanassi, D. G., Suh, G. S. & Nikaido, H. Role of outer membrane barrier in efflux-mediated
396 tetracycline resistance of *Escherichia coli*. *J Bacteriol* **177,** 998–1007 (1995).

397 43. Choi, U. & Lee, C.-R. Distinct Roles of Outer Membrane Porins in Antibiotic Resistance and
398 Membrane Integrity in *Escherichia coli*. *Front. Microbiol.* **10,** 953 (2019).

399 44. Delcour, A. H. Outer membrane permeability and antibiotic resistance. *Biochimica et*
400 *Biophysica Acta (BBA) - Proteins and Proteomics* **1794,** 808–816 (2009).

401 45. Tyson, J., Radford, P., Lambert, C., Till, R., Huwiler, S. G., Lovering, A. L. & Elizabeth
402 Sockett, R. Prey killing without invasion by *Bdellovibrio bacteriovorus* defective for a
403 MIDAS-family adhesin. *Nat Commun* **15,** 3078 (2024).

404 46. Varon, M. & Shilo, M. Attachment of *Bdellovibrio bacteriovorus* to cell wall mutants of
405 *Salmonella* spp. and *Escherichia coli*. *J Bacteriol* **97,** 977–979 (1969).

406 47. Schelling, M. & Conti, S. Host receptor sites involved in the attachment of *Bdellovibrio*
407 *bacteriovorus* and *Bdellovibrio stolpii*. *FEMS Microbiology Letters* **36,** 319–323 (1986).

408 48. Duncan, M. C., Forbes, J. C., Nguyen, Y., Shull, L. M., Gillette, R. K., Lazinski, D. W., Ali,
409 A., Shanks, R. M. Q., Kadouri, D. E. & Camilli, A. *Vibrio cholerae* motility exerts drag force
410 to impede attack by the bacterial predator *Bdellovibrio bacteriovorus*. *Nat Commun* **9,** 4757
411 (2018).

412 49. Wale, N., Sim, D. G., Jones, M. J., Salathe, R., Day, T. & Read, A. F. Resource limitation
413 prevents the emergence of drug resistance by intensifying within-host competition. *Proc. Natl.*
414 *Acad. Sci. U.S.A.* **114,** 13774–13779 (2017).

415

416

Acknowledgments

The authors would like to thank Dr. Timothy Sykes and Dr. Weihong Qi from Functional Genomics Center Zurich (FGCZ) for DNA library preparation, Illumina sequencing and initial data analysis by multi-sample variant calling. Microscopy images were obtained with a Leica Thunder microscope maintained by the Center for Microscopy and Image Analysis at University of Zurich. We would like to thank Prof. R. E. Sockett (University of Nottingham, UK) for providing *B. bacteriovorus* HD100^{T}. Further, we would like to thank Prof. Alex Hall and Dr. Daniel Angst (both ETH Zürich, CH) for the *E. coli* strains from the KEIO collection and pCP20. This study was enabled by FAN (Research Talent Development Fund of the University of Zurich Alumni), the Ernst Göhner Stiftung, as well as the Kurt und Senta Herrmann-Stiftung (all to S.M. and S.G.H.), all of which contributed towards research costs and salary of S.M.. R.K. was funded by a project grant from the Swiss National Science Foundation (no. 310030_212266), S.G.H. was funded by Swiss National Science Foundation Ambizione Fellowship PZ00P3_193401. A CC-BY-NC-ND copyright license is applied to this manuscript.

Author contributions

S.M. and S.G.H. jointly conceived the project and obtained funding with input from R.K. . S.M. and O.Ch.M. conducted the prey evolution experiment and isolated genomic DNA from prey populations for sequencing of ancestor and evolved prey lineages. S.M. and O.Ch.M. isolated single clones of evolved prey lineages and sent them for sequencing. S.M. and O.Ch.M. conducted predation assays with prey of ancestor and evolved lineage populations at the end timepoint (15th evolution cycle). S.M. made predation assays of evolved prey lineage populations at 2nd and 5th evolution cycles as well as evolved single clones (15th evolution cycle). S.L.L. performed predation assays of prey deletion strains with help of S.I. . Data analysis and evaluation of predation assays was done by O.Ch.M., S.L.L., and S.M. (lead). Genome sequence analysis was performed by O.Ch.M. (population), S.G.H. (population, gene mutations), S.L.L. (single clones, OmpF population mutations) and S.M. (population, single clones, all final heatmaps, lead). S.L.L. generated clean deletion strains Δ*ompF,* Δ*waaF,* Δ*envZ,* and Δ*truA.* S.I. and S.G.H. helped S.L.L. to generate Δ*waaB*. S.L.L. took microscopy images of prey ancestor and all evolved prey lineage populations (15th evolution cycle), as well as *E.coli* BW25113, Δ*envZ,* and Δ*truA*, with assistance of S.G.H. . S.L.L. performed image analysis with statistical input by S.M. . S.G.H. advised on predatory bacterial culturing, lab experimentation, prey sequencing, and molecular genetics aspects. R.K. advised on evolutionary and statistical aspects. S.M., S.G.H. and R.K.

wrote the paper with contributions from the other authors. All authors approved of the final version before submission.

Competing interests

The authors declare no competing interests.

Additional information

Extended data is available for this paper at https://doi.org/XXX.

Supplementary information The online version contains supplementary material available at https://doi.org/XXX.

Requests for materials should be addressed to Simona G. Huwiler.

Main figures

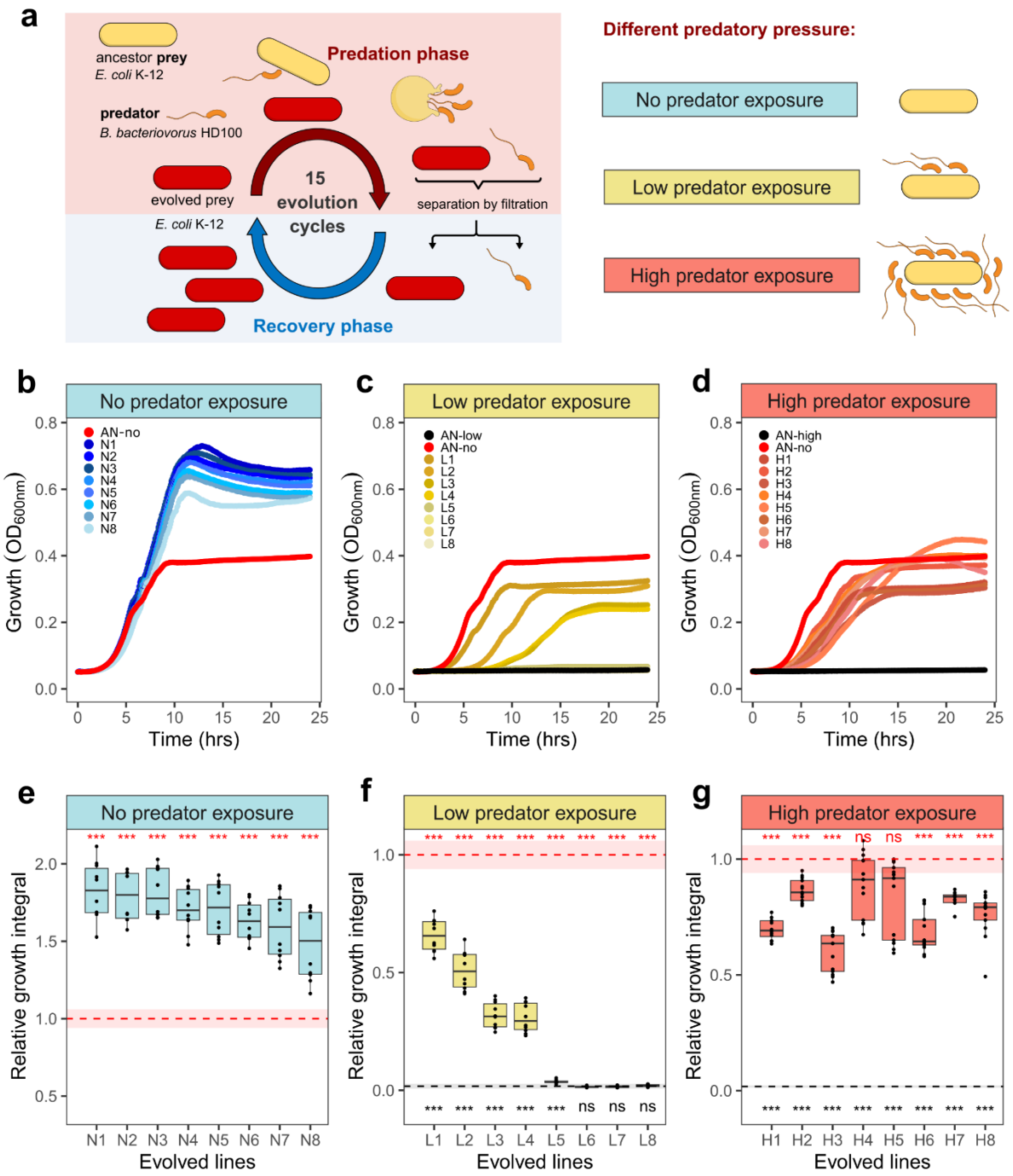

Fig. 1 | Repeated exposure of predator *B. bacteriovorus* HD100 leads to growth of prey *E. coli* K-12 under predation. a, Experimental evolution scheme: eight different prey lineages are exposed repeatedly to different concentration of the predator: no (N1-N8, blue), low (L1-L8, yellow) and high (H1-H8, red) predatory pressure. Each prey evolution cycle is composed of an alternating predation and recovery phase, whereby surviving prey is separated, recovered and re-exposed to predation for 15 cycles. Growth dynamics of evolved prey from 15th cycle: **b-d,** growth curves measured as OD_{600nm}

488 over time of eight independently evolved prey lineages under no (b), low (c) and high (d) predatory
489 pressure when exposed to respective predation conditions where they evolved. They were compared with
490 ancestor under no (AN-no) or specific predatory pressures (AN-low & AN-high). Each point of the
491 growth curves represents average OD_{600nm} at that timepoint across replicates. **e-g,** Relative growth
492 integral of **b-d**, defined as growth integral (area under the curve) divided by the growth integral of
493 ancestor under no predatory pressure. Boxplots represent the median with 25th and 75th percentiles, and
494 whiskers show the 1.5 interquartile range. Red dotted line and shadow indicate the mean and standard
495 deviation range of AN-no. Black dotted lines and shaded areas indicate the mean and standard deviation
496 range of AN under respective predation conditions. The p-value significance levels (two-sided one
497 sample t-tests, $p>0.05$ = ns, $p<0.05$ = *, $p<0.01$ = **, $p<0.001$= ***) in comparison to AN-no is shown
498 by red asterisks and comparison to ancestor under respective predatory pressures are shown by black
499 asterisks. Experiments were repeated independently at least twice, N1-8 (n = 10 replicates), L1-8 (n =
500 10 replicates), H1-8 (n = 13 replicates), AN-no (n = 72 replicates), AN-low (n = 10 replicates) and AN-
501 high (n = 62 replicates).

502

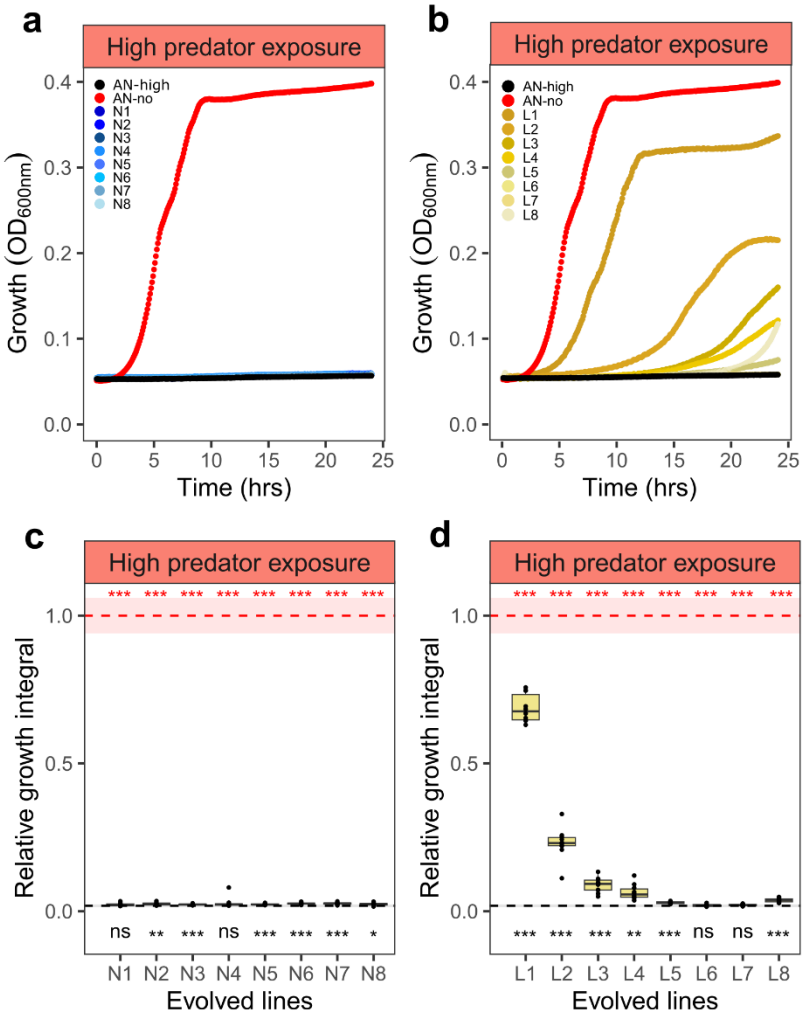

Fig. 2 | Predation resistance evolves only under predation. Growth dynamics of evolved prey from 15th cycle: **a** & **b**, growth curves measured as OD_{600nm} over time of eight independently evolved prey lineages under no (a, N1-8, blue) and low (b, L1-8, yellow) predatory pressure when exposed to high predatory pressure and compared with ancestor population under no (AN-no, red line) and high (AN-high, black line) predatory pressure. Each point of the growth curves represents average OD_{600nm} at that timepoint across replicates. **c** & **d**, Relative growth integral of **a** & **b**, defined as growth integral (area under the curve) divided by the growth integral of AN-no. Boxplots represent the median with 25th and 75th percentiles, and whiskers show the 1.5 interquartile range. Dotted lines and shaded areas indicate the mean and standard deviation range of the ancestor under no (AN-no, red) and high (AN-high, black) predatory pressure. The p-value significance levels (two-sided one sample t-tests, $p>0.05$ = ns, $p<0.05$ = *, $p<0.01$ = **, $p<0.001$= ***) in comparison to AN-no are shown by red asterisks, and to AN-high are shown by black asterisks. Experiments were repeated independently at least twice, N1-8 (n= 10 replicates), L1-8 (n= 10 replicates), AN-no (n= 72 replicates), and AN-high (n= 62 replicates).

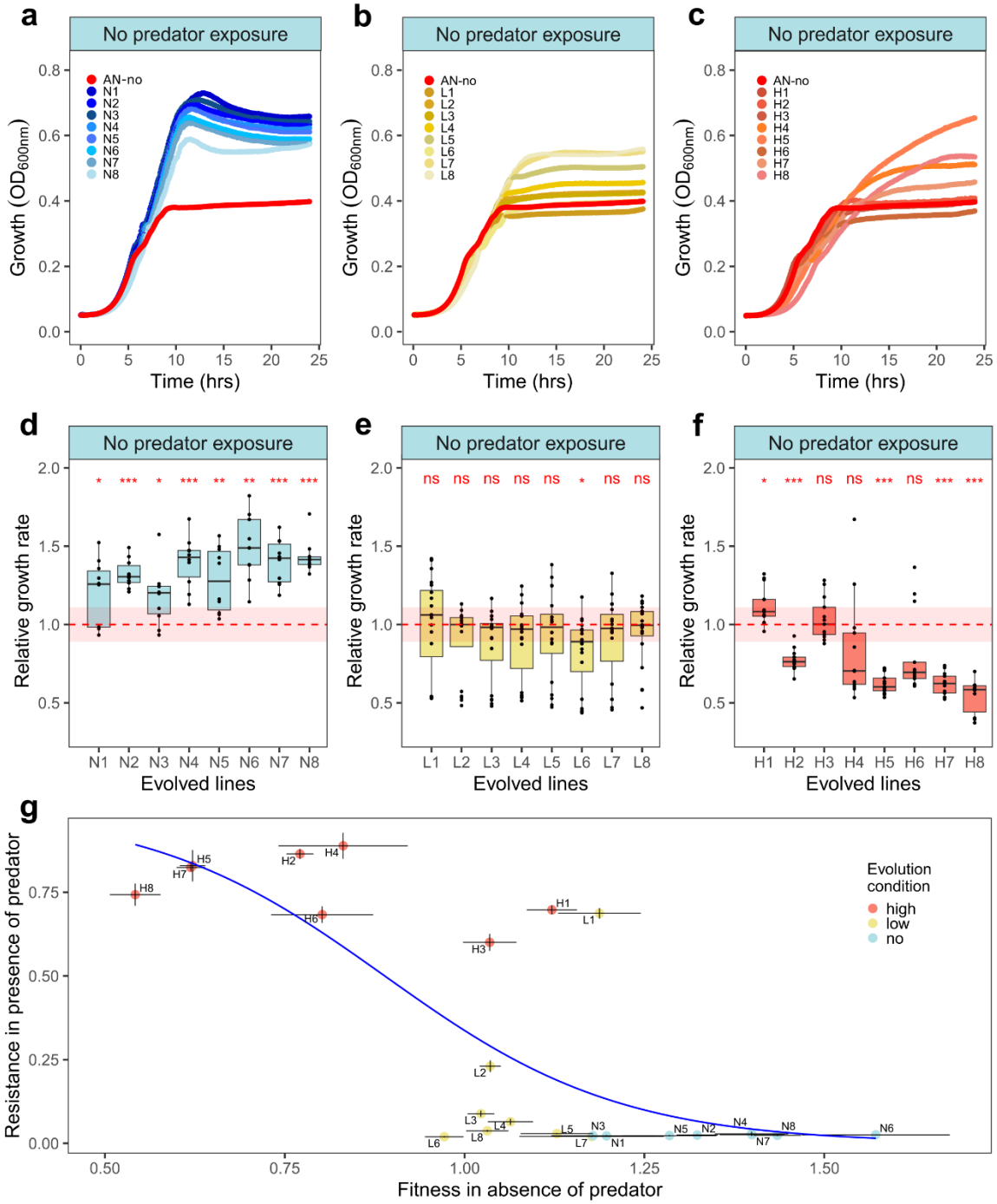

Fig. 3 | Prey resistance to bacterial predator is generally associated with negative fitness consequences. Growth dynamics of evolved prey from 15th cycle: **a-c** growth curves measured as OD600nm over time, of prey lineages evolved under no (**a,** blue), low (**b,** yellow) and high (**c,** salmon) predatory pressure, when exposed to no predatory pressure. Each point of the growth curve represents the average OD600nm at that timepoint across replicates. Panel **a** is identical with Fig. 1a for a complete overview. **d-f,** Relative growth rates of no (**d**), low (**e**), and high (**f**) predatory pressure evolved lines, when exposed to no predatory pressure. Relative growth rate is defined as maximum growth rate divided by the maximum growth rate of the ancestor under no predatory pressure (AN-no).

555 Boxplots represent the median with 25th and 75th percentiles, and whiskers show the 1.5 interquartile
556 range. Red dotted lines and shaded areas indicate the mean and standard deviation range of ancestor
557 under no predatory pressure (AN-no). The p-value significance levels (two-sided one sample t-tests,
558 $p>0.05$ = ns, $p<0.05$ = *, $p<0.01$ = **, $p<0.001$ = ***) in comparison to AN-no are shown by red
559 asterisks. Experiments were repeated independently at least twice, N1-8 (n= 10 replicates), L1-8 (n=
560 20 replicates), H1-8 (n= 13 replicates), AN-no (n= 72 replicates). Three outliers, one each from N6,
561 L4 and L7 were excluded from panels **d & e** for better visualisation but were included in the statistical
562 analysis. **g,** Trade-off between predation resistance and prey fitness. Fitness, quantified as mean
563 relative growth rate under no predatory pressure (**d-f**) versus predator resistance, quantified as mean
564 relative growth integral under high predatory pressure (Fig. 1g & 2c-d). N1-8, L1-8, and H1-8 denotes
565 prey lineages that evolved under no (blue), low (yellow) and high (salmon) predatory pressure
566 respectively. A logistic regression function was fitted as a blue line to correlate the two variables
567 (resistance versus fitness, Wald z-statistics = -2.336, p- value = 0.0195). Black error bars represent the
568 standard error of mean for the respective variables.

569

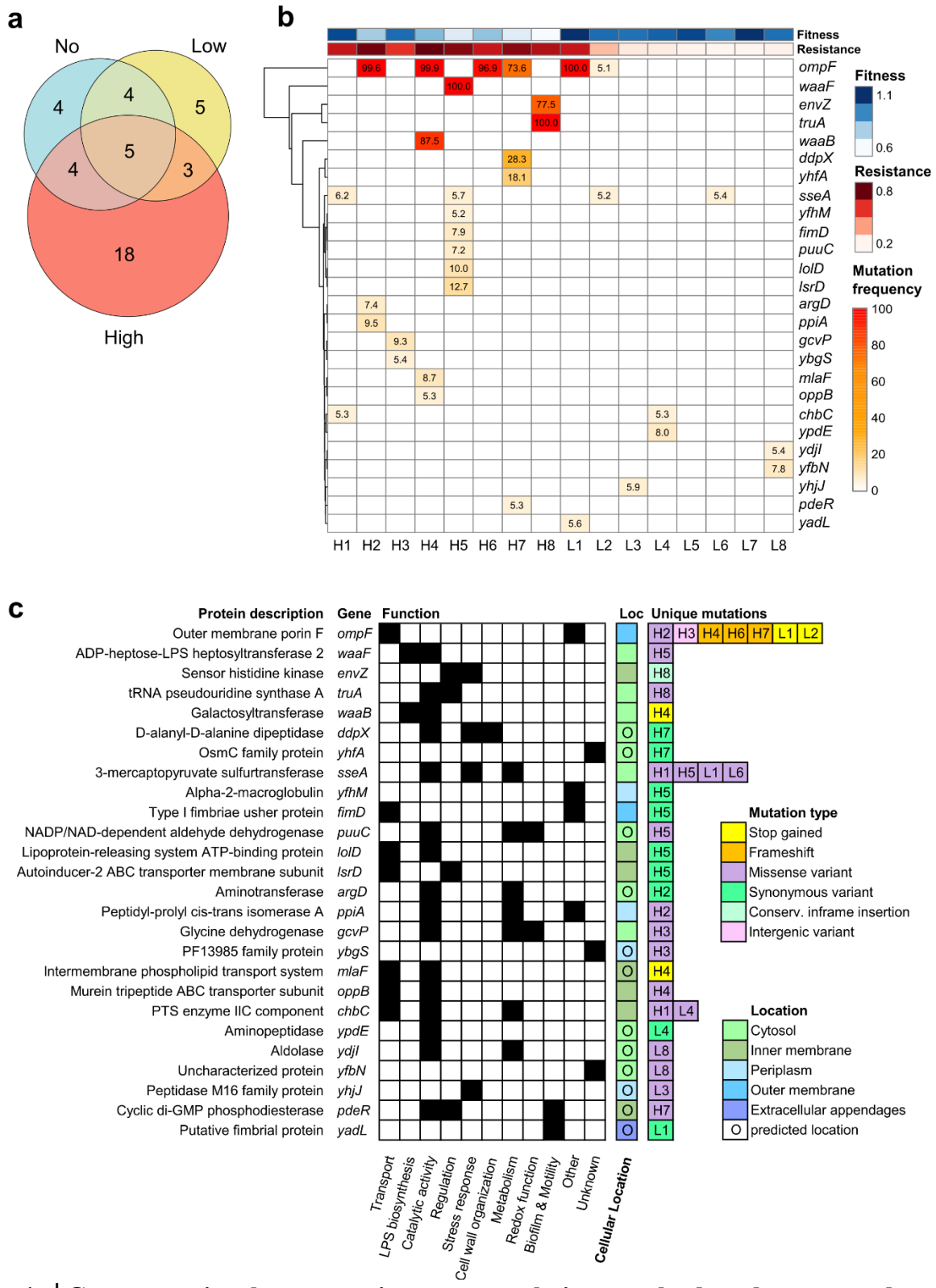

Fig. 4 | Gene mutational patterns in prey populations evolved under repeated predation pressure. Genes mutated in evolved *E. coli* K-12 lineages after the 15th evolution cycle in comparison to the ancestor. **a,** Venn diagram showing the number of mutated *E. coli* genes that reached frequencies higher than 5% within a lineage, grouped according to no, low and high predatory pressure. Not

593 included in this Venn diagram are mutated rRNA and transposase genes, which are listed separately
594 (Extended Data Fig. 7). **b**, Hierarchically clustered heatmap of mutation frequency differences relative
595 to the ancestor of all the genes that exclusively mutated under high (H1-8) and/or low (L1-8) predatory
596 pressure. Heatmaps on top of the panel show fitness (blue) measured as average relative growth rate
597 of lineages under no predatory pressure, and resistance (red) measured as average relative growth
598 integral of lineages under high predatory pressure, according to the data in Fig. 3g. **c**, Overview of
599 mutated genes and mutation types together with a description of the encoded proteins, their functions
600 and cellular location (Loc) for all the genes that exclusively mutated under high and/or low predatory
601 pressure, according to **b**.

602

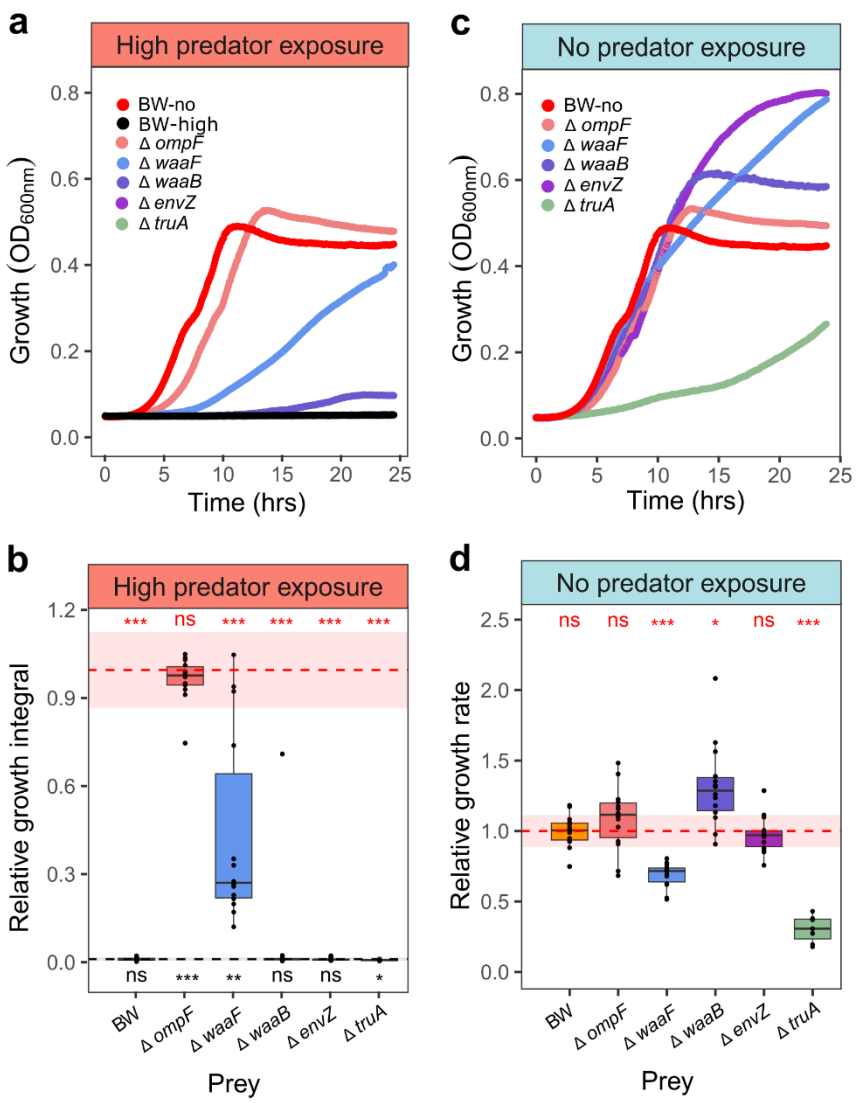

Fig. 5 | OmpF deletion in *E. coli* prey results in high predation resistance. Different *E. coli* clean-deletion mutant strains (Δ*ompF*, Δ*waaF*, Δ*waaB*, Δ*envZ*, Δ*truA*) were generated based on the KEIO library. *E. coli* BW25113 (BW) is the KEIO reference strain. **a+c**, Growth curves measured as OD_{600nm} over time of the different *E. coli* deletion mutants exposed to either high predatory pressure (**a**) or no predators (**c**). Each point of the growth curve represents the average OD_{600nm} per timepoint across replicates. Experiments were independently repeated at least twice. Total replicate numbers for the various strains: Δ*ompF* (n= 14), Δ*waaF* (n= 14), Δ*waaB* (n= 14), Δ*envZ* (n= 14), Δ*truA* (n= 8), BW without predatory pressure (BW-no) (n= 14), and BW with high predatory pressure (BW-high) (n= 15). **b,** Relative growth integrals from **a**. Relative growth integrals are calculated as growth integral (area under the curve) of the clean-deletion mutant with predatory pressure divided by the growth integral of BW-no. **d**, Relative growth rates from **c**. Relative growth rates are calculated as the maximum growth rate of the clean-deletion mutant divided by the maximum growth rate of BW-no .

Boxplots represent the median with 25th and 75th percentiles, and whiskers show the 1.5 interquartile range. Red and black dotted lines and shaded areas indicate the mean and standard deviation range of BW-no and BW-high respectively. The p-value significance levels (two-sided one sample t-tests, $p>0.05$ = ns, $p<0.05$ = *, $p<0.01$ = **, $p<0.001$= ***) in comparison to BW-no (red asterisks), and to BW-high (black asterisks).

635 # Methods

636 **Growth of bacterial strains**

637 In this study, *Escherichia coli* K-12 MG1655 (DSM 18039) as prey and *Bdellovibrio bacteriovorus*
638 HD100^T as predator were used, unless indicated otherwise. *B. bacteriovorus* HD100^T was obtained
639 from the laboratory of Prof. R. E. Sockett at University of Nottingham, UK. *B. bacteriovorus* HD100
640 was cultured and maintained on Ca/HEPES buffer (25 mM HEPES, 2 mM $CaCl_2$, pH 7.6) with late-
641 log *E. coli* K-12 MG1655 at 29°C for generally 24 h at 200 rpm shaking[1]. General revival of
642 *B. bacteriovorus* and determination of plaque forming units (PFU) for enumeration was done according
643 to protocols by Lambert & Sockett[1] and is described in more detail at the end of the Additional Online
644 materials.

645 All *E. coli* strains used are listed in Additional Online Materials Table SOnline1. To validate the
646 genetic effect on predation resistance, markerless single deletion strains Δ*envZ,* Δ*ompF,* Δ*truA,* Δ*waaB,*
647 and Δ*waaF* were generated based on *E.coli* KEIO library strains[2] containing an inserted kanamycin
648 resistance cassette (following section). The different *E. coli* strains were generally grown in YT both
649 (Yeast tryptone, 5 g l^{-1} NaCl, 5 g l^{-1} Bacto yeast extract, 8 g l^{-1} tryptone, pH 7.5) at 37°C with 200 rpm
650 shaking for generally 16 h overnight, and additional appropriate antibiotics as indicated. For ancestor
651 prey, *E. coli* K-12 MG1655 was retrieved from 20% glycerol stocks at -80°C and were streaked on a
652 YT agar plate (YT broth with 10 g l^{-1} agar) and incubated at 37°C for 24 h to obtain single colonies.
653 The overnight cultures from ancestor prey single colonies were used for 24-hr lysates (growth of
654 predator), revival and enumeration of the predator in our experiments.

655

656 **Generation of markerless deletion strains of *E. coli* KEIO library**

657 Markerless single deletion mutants in *E. coli* (Δ*envZ,* Δ*ompF,* Δ*truA,* Δ*waaB,* and Δ*waaF*) were
658 constructed of the respective strain from the KEIO collection (based on *E. coli* BW25113)[2]. To achieve
659 this, the kanamycin resistance cassette (present in the KEIO collection to disrupt the individual genes)
660 was removed to enable predation assays with kanamycin-sensitive *B. bacteriovorus* HD100. The
661 kanamycin cassette was excised via pCP20[3], expressing an FLP-FRT recombinase. To generate
662 electrocompetent cells, and excise the kanamycin cassette, several protocols from the Barrick lab were
663 adapted[4,5]. To prepare electrocompetent cells the desired *E. coli* strain in YT broth with 30 µg/ml

664 kanamycin was incubated for 16 h at 37°C and 200 rpm. The stationary phase culture was used to
665 inoculate at least 10 ml of YT broth with 30 µg/ml kanamycin at optical density with absorbance at
666 600nm (OD_{600nm}) of 0.05 and grown at 37°C and 200 rpm. At an OD_{600nm} of ~ 0.6 the culture was
667 centrifuged for 5 minutes at 6000 x *g* and 4°C, and the supernatant was discarded. The resulting pellet
668 was washed 4 times with 10% ice-cold glycerol of the same volume as the initial inoculation volume.
669 Finally, the pellet was resuspended in 10% glycerol at 100x concentration, and 50 µl aliquots stored at
670 -80°C. These electrocompetent *E. coli* cells were thawed on ice and maximally 100 ng of pCP20 added.
671 After gentle mixing, the sample was transferred into a cooled 0.2-cm cuvette (Bio-Rad), and
672 electroporated at 2.5 kV with a MicroPulser electroporator (Bio-Rad). Then, the sample was
673 resuspended in 500 µl warm SOC medium and incubated for 30 min at 30°C and 120 rpm. The cells
674 were plated on YT agar plates with 100 µg/ml ampicillin and grown at 29°C for at least 16 h. To select
675 for loss of heat-sensitive plasmid pCP20 after recombination, a single colony from a YT agar plate
676 with 100 µg/ml ampicillin was picked to inoculate 5 ml of YT broth, and grown for 16 h at 43°C,
677 shaking at 200 rpm. 50 µl of a 10^{-6} dilution of this stationary phase culture was plated on YT agar
678 without antibiotics for single clones. To screen for successful recombination and loss of plasmid, six
679 colonies were selected and streaked out on YT agar with 30 µg/ml kanamycin, YT agar with 100 µg/ml
680 ampicillin, and YT agar without antibiotics in this order. The YT plates without and with kanamycin
681 were incubated at 37°C, the YT plates with ampicillin at 29°C for at least 16 h. To screen for successful
682 excision of the kanamycin cassette, recombinants with sensitivity to both antibiotics were grown in
683 5 ml of YT broth, incubated for 16 h at 200 rpm and 37°C. Of these cultures, 20% glycerol stocks were
684 made and stored at -80°C. To control correct excision of the kanamycin cassette, PCR was used to
685 assess correct product size (Primers in Additional Online Materials Table SOnline 2). Additionally,
686 correct scar regions were confirmed by sanger sequencing (Microsynth AG, CH).

687

688 **Experimental prey evolution**

689 In the experimental prey evolution, *E. coli* K-12 MG1655 was used as ancestral prey strain and
690 subjected to three different predatory pressures by *B. bacteriovorus* HD100 involving 15 alternate
691 cycles of predation and recovery phase (Fig. 1a). The detailed protocol is described at the end of the
692 Supplementary Online Materials. The predation phase occurred in rich medium (containing ¾ YT, 1/4
693 25 mM HEPES and 2 mM $CaCl_2$) allowing growth of *E. coli* K-12 as well as predation of
694 *B. bacteriovorus* at 200 rpm and 29°C. *E. coli* K-12 prey were subjected to three different predatory

695 conditions: No predatory, low predatory pressure (multiplicity of infection [MOI], ratio of predator
696 (PFU/ml) vs prey cells (CFU/ml), was ~ 2.5) and high predatory pressure (MOI ~10). For each
697 condition eight independent prey lineages were evolved from the *E. coli* K-12 ancestor. After the 24-
698 hr predation phase surviving *E. coli* were separated from *B. bacteriovorus* by filtration to avoid co-
699 evolution. In the subsequent 16-hr recovery phase retrieved *E. coli* from filtration were diluted ~1:100
700 and grown in YT at 200 rpm and 37°C. These overnight cultures were diluted back to an overall initial
701 OD_{600nm} of 0.003 for the next predation phase and evolution cycle.

702

703 **Isolation of prey single clones**

704 Prior to the experiment we made overnight cultures of evolved lineages under high predatory pressure
705 (15th evolution cycle) stored at -80°C, by extracting cell material (containing evolved population) from
706 cryo stocks and inoculating 50 ml YT medium in 250 ml Erlenmeyer flasks, incubated at 37°C,
707 200 rpm for 16 h. We harvested prey cells from 10ml of these overnight cultures by centrifugation at
708 5311 x *g* for 3 min and subsequently washed them in 10 ml of Ca-HEPES. Then prey cells were
709 resuspended in 6 ml of Ca-HEPES and adjusted to $OD_{600nm} = 3.0$, then we diluted the cultures to 10^{-6}
710 and plated 100 µl on YT agar plates and incubated them at 37°C for 24 h. We randomly selected 6
711 single colonies from each evolved lineage and overnight cultures were made with these single colonies
712 in 10 ml YT medium in 50 ml Falcon tubes incubated at 37°C, 200 rpm for 16 h. From this culture we
713 prepared 20% glycerol stocks and stored them at -80°C. Prior to experiments, we made overnight
714 cultures of the single colonies from cryo stocks, alongside their respective evolved lineage population
715 and ancestor in 50 ml YT medium in 250 ml Erlenmeyer flasks, incubated at 37°C, 200 rpm for 16
716 hours. These single clone cultures were used for predation assays and genome sequencing.

717

718 **Predation assay**

719 To evaluate predation resistance and growth dynamics of different prey, predation assays were
720 performed. Different *E. coli* prey strains were assessed: *E. coli* K-12 MG1655 population lineages
721 evolved under high (H1-8), low (L1-8) and no (N1-8) predatory pressure at the end 15th evolution cycle
722 (after recovery phase) were compared with ancestor *E. coli* K-12 MG1655. At first, we exposed prey

723 lineages that evolved under a particular predatory pressure to that pressure. We then focussed on
724 exposing evolved lines to the high predatory pressure condition.

725 To investigate the temporal aspect of evolution, we performed predation assays of prey lineages
726 evolved under high predatory pressure (H1-H8) at the end of the 2nd and 5th evolution cycle and
727 compared them to the 15th cycle, when exposed to high predatory pressure. To test for cross resistance,
728 we assessed the performance of prey that evolved under no or low predator by exposing them to high
729 predatory pressure. The predation assays at the population level featured 5 replicates per prey-predator
730 combination and were repeated on two separate days.

731 To assess effects of specific prey genes on predation resistance, predation assay was conducted with
732 markerless single gene deletion mutants (Δ*envZ,* Δ*ompF,* Δ*truA,* Δ*waaB,* and Δ*waaF* based on *E. coli*
733 BW25113 (reference strain from KEIO library[2]). These strains were exposed to high and no predatory
734 pressure conditions.

735 Prior to the predation assay, respective evolved prey lineages or prey strains (evolved lineages,
736 population- or single clone-based, single gene deletion, and KEIO reference strain) were grown from
737 cryo stocks by inoculation in 50 ml YT broth and incubation at 37°C and 200 rpm for 16 h.
738 Additionally, an overnight culture of ancestor prey was prepared from a single colony, at same growth
739 conditions. The eight independently evolved prey lineages under each predatory pressure were assessed
740 in parallel alongside ancestor prey. 10-ml prey overnight cultures were centrifuged at 5311 x *g* for 3
741 min and subsequently washed with 10 ml of Ca-HEPES buffer. Then prey cells were resuspended in
742 6 ml of Ca-HEPES buffer and adjusted to OD_{600nm} = 0.03. A 24-hr predator lysate was filtered through
743 a 0.8-µm syringe filter (Whatman® Puradisc FP 30, Cellulose Acetate, sterile, WHA10462240). For
744 the predation assays, the same cultivation media was used as for the experimental evolution predation
745 phase, comprising 15 ml of YT broth, 5 ml of 25 mM HEPES and 2 mM $CaCl_2$ overall. We set up the
746 predation assay in 96-well plates, in a total volume of 150 µl. Initially 119 µl of cultivation media was
747 preset, and different volumes of the filtered predator lysate were added to the assay: 0 µl (no predator
748 exposure), 4 µl (low predator exposure) or 16 µl (high predator exposure), depending on the evolved
749 prey lineages and predatory pressure tested. Then we added 15 µl of the respective prey solution
750 (OD_{600nm} = 0.03 in Ca-HEPES). Then we adjusted the final volume in reaction wells to 150 µl by
751 adding Ca-HEPES (as proxy for predator lysate and prey resuspension), resulting in a final
752 concentration of prey of OD_{600nm} = 0.003. We used the same ratio of prey and predator as in the

753 predation phase of the prey evolution experiment. The plate was incubated in a plate reader (Tecan
754 Infinite 200 Pro) at 29°C for 24 h. OD_{600nm} of the reaction wells was measured with 10 flashes every
755 5 minutes after shaking at 6-mm amplitude for 120 secs.

756 We used OD_{600nm} as proxy for the biomass of prey cells, as the predator cells only contribute to a very
757 minor fraction to OD_{600nm} based on the small size. The kinetic measurement of OD_{600nm} over 24 h, was
758 analysed using an interactive platform for analysis of microbial growth data
759 (https://statu.shinyapps.io/ExploreMicrobialGrowth/, version 2016.01.12) designed by Adin Ross-
760 Gillespie at University of Zurich. We used Spline function to fit the kinetic growth data to extract the
761 integral (area under the curve) and maximal growth increase rate. For the predation assays in cultivation
762 media, we derived relative growth integral and growth rate of evolved prey lineages in comparison to
763 the ancestor prey. For this we divided the growth integral or growth rate of evolved lineages under all
764 predator conditions by that of ancestor when exposed to no predator, that is baseline. Values > 1 or <
765 1, indicate that evolved lineages perform better or worse than baseline.

766

767 **Cell shape analysis by phase-contrast microscopy**

768 *E. coli* K-12 lineages evolved under low, no, and high predatory pressure at the end of experimental
769 evolution (after the 15th evolution cycle), *E. coli* K-12 MG1655 (ancestor), as well as *E. coli* K-12
770 BW25113, Δ*envZ* and Δ*truA* were regrown from cryo stocks in YT broth at 37°C and 200 rpm shaking
771 overnight. From each culture 10 µl was applied onto a 1% agarose in Ca/HEPES buffer pad on a clean
772 microscope slide for phase-contrast microscopy. Imaging was performed using a Leica DMi8 inverted
773 microscope equipped with a 100x objective (HC PL APO 1.40 oil PH3), a Leica monochrome
774 fluorescence DFC9000 gTC Camera System, and Leica Application Suite X Software Version
775 3.7.6.25997 (Leica microsystems). Exposure time was 100 ms with illumination intensity of 140. For
776 each evolved lineage and ancestor strain *E. coli* K-12 MG1655 a minimum of 15 images were
777 collected. For shape analysis of the evolved cells, software Fjij/ImageJ (Version 2.90/1.53t, Java
778 1.8.0322, 64-bit)[6,7] was used with the Plugin MicrobeJ (Version 5.13o (16) – beta)[8]. Area and length
779 restrictions were set to 0.5-3 p^2, width to 0.5-2 p^2. After initial shape detection, masks were manually
780 adjusted to observed cell size and a minimum of 300 cells per lineage/strain were analysed.

781

782 **Statistical analyses**

783 We used general linear models for statistical analysis in R 4.2.3[9,10]. To assess whether relative growth
784 integral and relative growth rate vary in response to predatory pressure we used analysis of variance
785 (ANOVA) models (Fig. 1e-g, Fig. 2 c,d & Fig. 3d-f). We further used two-sided one-sample *t*-tests to
786 test for significant differences in relative growth integral or growth rate between evolved prey lineages
787 and that of ancestor when exposed to either no, low or high predatory pressure (i.e. being different
788 from mean relative growth integral or growth rate of ancestor, Fig. 1e-g & Fig. 2c-d & Fig. 3d-f & Fig.
789 5b,d & Extended Data Fig. 2d-f, j-l). Reported p-values for *t*-tests were adjusted for multiple testing
790 using the Holm method. We used a logistic regression model to test for a negative association (tradeoff)
791 between mean relative growth integral and mean relative growth rate (Fig. 3g). A detailed statistical
792 output of the data of this article is available in an Additional Online Material table.

793

794 **Genome sequencing and analysis of evolved prey population lineages**

795 We sequenced the genome of the 24 prey lineages (i.e. population) that evolved under no, low and high
796 predatory pressure condition (8 each) after the 15th evolution cycle, at the population level and
797 compared it with the ancestor prey genome. Overnight cultures were grown in YT broth (200 rpm at
798 37°C) from cryo stocks of evolved prey lineages from the 15th recovery phase at the end of
799 experimental evolution and separately from a single colony of the ancestor prey. From these cultures
800 we extracted genomic DNA using GenElute^{TM} Bacterial Genomic DNA Kit (Sigma, NA2110). The
801 concentration of genomic DNA varied between 83.77 to 205. 407 ng/µl, which was sufficient for
802 standard library preparation. The samples were then transferred to the Functional Genomic Center
803 Zurich (FGCZ, Switzerland) for sequencing and base variant calling of the sequencing data of evolved
804 lineages against the ancestor. For library preparation the TruSeq DNA Nano Sample Prep Kit v2
805 (Illumina, Inc, California, USA) was used in the succeeding steps. DNA samples (100ng) were
806 sonicated with the Covaris using settings specific to the fragment size of 350 bp. The fragmented DNA
807 samples were size- selected using AMpure beads, end-repaired and adenylated. TruSeq adapters
808 containing Unique Dual Indices (UDI) for multiplexing were ligated to the size-selected DNA samples.
809 Fragments containing TruSeq adapters on both ends were selectively enriched by PCR. The quality
810 and quantity of the enriched libraries were validated using TapeStation (Agilent, Waldbronn,
811 Germany). An average fragment size of approximately 500 bp was achieved. The libraries were

812 normalized to 10 nM in Tris-Cl 10 mM, pH 8.5 with 0.1% Tween 20. For sequencing and cluster
813 generation the Novaseq 6000 (Illumina, Inc, California, USA) was used according to standard protocol.
814 Sequencing were paired end at 2 X150 bp. Technical quality of Illumina paired-end (PE) reads was
815 evaluated using FastQC (v0.11.9) and FastQScreen (v0.14.1). Raw reads were pre-processed using
816 fastp (v0.20.0) with the following parameter: hard trimming of 10 nucleotide (nt) and 1 nt at 5' and 3
817 ends, respectively; quality trimming of both ends using a sliding window of 4 nt and mean quality of
818 20; trimmed reads shorter than 18 nt, and trimmed reads with mean read quality lower than 20 were
819 filtered out. Pre-processed PE reads were aligned to the reference genome (*E. coli* K-12 MG1655 refseq
820 GCF_000005845.2) using bwa (v0.7.17) with the "mem" algorithm. PCR duplicates were marked
821 using Picard (v2.22.8, MarkDuplicates). Mapping results were quality controlled using SAMStat
822 (v1.5.1), Qualimap (v2.2.1), and Picard (v2.22.8, CollectGcBiasMetrics). Multi-sample variant calling
823 was performed using freebayes (V1.3.2) with frequency cutoffs of 5% and 1%, respectively. Only
824 unique reads in primary alignments with alignment quality 30 and above, and bases with quality 20
825 and above, were counted for variant analysis. Sites with multiple alternative alleles were split into
826 multiple rows using bcftools. Variant annotation was performed using snpEff (v4.3) against reference
827 gene models (NCBI, reference genome: ASM584v2, refseq: GCF_000005845.2). Called variants were
828 filtered against the ancestor strain using a customized Perl script. Markers were retained, where all
829 counted reads contain only the reference alleles in the ancestor strain. Per sample variant frequencies
830 were then calculated for these markers using the customized Perl script. The resulting excel file from
831 population variant calling was used for further analysis and representation by hierarchically clustered
832 heatmaps on absolute mutation frequencies and their differences compared to the ancestor strain.
833 Heatmaps were generated in R with Pheatmap[11]. We focused on gene mutations with a frequency more
834 than 5%. If a particular gene had multiple mutation effects, we selected the mutation with the highest
835 frequency. Mutation counts were added to a gene only if the mutation was located within the coding
836 region of a specific gene (direct effects). This excludes downstream effects on adjacent genes.
837 Mutations lying in intergenic regions were ignored due to their ambiguous impact on surrounding
838 genes. An exception was made for the mutation located in the intergenic region between *asnS* and
839 *ompF*. Since it is located 143 bp upstream the *ompF* transcription start site various *ompF* regulators
840 bind adjacent to this locus and is likely to influence *ompF* transcription. The mutations in *ompF* were
841 analysed in detail and the OmpF amino acid sequence with changes in the different prey lineages was
842 constructed in Excel (Microsoft Corporation, 2018) and compared with the ancestor strain. Uniquely
843 mutated genes (without transposases and rRNA genes) of all genomes of prey lineages at the respective
844 predatory pressure were plotted using R package VennDiagram[12].

845

846 **Genome sequencing and variant calling for prey single clones**

847 48 cultures were prepared from six single prey clones each of all eight prey lineages evolved under
848 high predatory pressure (H1-H8) at the end of the 15th evolution cycle. Overnight cultures of these
849 single clones from lineages evolved under high-predatory pressure were inoculated from cryo stocks
850 into 10 ml YT medium in 50 ml Falcon tubes, and incubated at 37°C, 200 rpm for 16 h. We harvested
851 prey cells equivalent of OD_{600nm} = 10.0 from these cultures by centrifugation at 5000 *g* for 5 min, the
852 cells were then washed (5000 g for 5 minutes) in 1 ml Phosphate buffered saline (Gibco) and
853 resuspended into 0.5ml DNA/RNA shield buffer (Zymo Research). This mixture was sent to
854 MicrobesNG (UK, https://microbesng.com, Birmingham, UK), for DNA extraction, sequencing and
855 base variant calling against reference genome *E. coli* K-12 MG1655.

856 DNA was extracted by lysing 4-5 µl cell suspension with 120 µL of TE buffer containing lysozyme
857 (MPBio, USA), metapolyzyme (Sigma Aldrich, USA) and RNase A (ITW Reagents, Spain), and
858 incubated for 25 min at 37°C. Proteinase K (VWR Chemicals, Ohio, USA) (final concentration
859 0.1mg/mL) and SDS (Sigma-Aldrich, Missouri, USA) (final concentration 0.5% v/v) are added and
860 incubated for 5 min at 65°C. Genomic DNA was purified using an equal volume of SPRI beads and
861 resuspended in EB buffer (10mM Tris-HCl, pH 8.0). The DNA was quantified with the Quant-iT
862 dsDNA HS (ThermoFisher Scientific) assay in an Eppendorf AF2200 plate reader (Eppendorf UK Ltd,
863 United Kingdom) and diluted as appropriate. Genomic DNA libraries are prepared using the Nextera
864 XT Library Prep Kit (Illumina, San Diego, USA) following the manufacturer's protocol with the
865 following modifications: input DNA is increased 2-fold, and PCR elongation time is increased to
866 45 sec. DNA quantification and library preparation are carried out on a Hamilton Microlab STAR
867 automated liquid handling system (Hamilton Bonaduz AG, Switzerland). Libraries are sequenced on
868 an lllumina NovaSeq 6000 (Illumina, San Diego, USA) using a 250 bp paired end protocol. For projects
869 predating April, 2020, libraries were sequenced on an Illumina HiSeq 2500 using a 250 bp paired-end
870 protocol (Illumina, San Diego, USA). Reads are adapter trimmed using Trimmomatic version 0.30 [13]
871 with a sliding window quality cutoff of Q15. De novo assembly is performed on samples using SPAdes
872 version 3.7 [14], and contigs are annotated using Prokka version 1.11 [15]. Reads were aligned to the
873 reference using BWA mem v0.7.17 [16] and are then processed using SAMtools v1.9 [17]. Variants were
874 called using VarScan v2.4.0 [18] with two thresholds, sensitive and specific, where the variant allele
875 frequency is greater than 10% respectively. The effects of the variants are predicted and annotated

using SnpEff v4.3 [19]. The base variant calling was performed using the criteria of a sequence coverage of at least 3x and a frequency of at least 10% to generate a table reporting on the differences to the reference genome (NCBI, refseq: GCF_000005845.2). The resulting Microsoft Excel table obtained from Microbes NG was used to combine it with the population sequencing data based on the nucleotide position. Gene annotations were obtained from both population and clone sequencing data, with frequency more than 5%.

Data availability. The raw data (OD_{600nm} measurements over time, microscopy images and raw data on width and length, R code used for analysis) used to generate the findings of this project have been deposited in the figshare repository (doi: XXX). The sequencing data for this study has been deposited in the European Nucleotide Archive (ENA) at EMBL-EBI under accession number PRJEB78919 (https://www.ebi.ac.uk/ena/browser/view/PRJEB78919).

References (Methods):

1. Lambert, C. & Sockett, R. E. Laboratory maintenance of Bdellovibrio. *Curr Protoc Microbiol* Chapter **7,** Unit 7B.2 (2008).

2. Baba, T., Ara, T., Hasegawa, M., Takai, Y., Okumura, Y., Baba, M., Datsenko, K. A., Tomita, M., Wanner, B. L. & Mori, H. Construction of *Escherichia coli* K-12 in-frame, single-gene knockout mutants: the Keio collection. *Molecular Systems Biology* **2,** 2006.0008 (2006).

3. Datsenko, K. A. & Wanner, B. L. One-step inactivation of chromosomal genes in *Escherichia coli* K-12 using PCR products. *Proc. Natl. Acad. Sci. U.S.A.* **97,** 6640–6645 (2000).

4. Barrick Lab. Barrick Lab :: ProtocolsElectrocompetentCells. at <https://barricklab.org/twiki/bin/view/Lab/ProtocolsElectrocompetentCells>

5. Barrick Lab. Barrick Lab :: ProcedureFLPFRTRecombination. at <https://barricklab.org/twiki/bin/view/Lab/ProcedureFLPFRTRecombination>

902 6. Schindelin, J., Arganda-Carreras, I., Frise, E., Kaynig, V., Longair, M., Pietzsch, T., Preibisch,
903 S., Rueden, C., Saalfeld, S., Schmid, B., Tinevez, J.-Y., White, D. J., Hartenstein, V., Eliceiri,
904 K., Tomancak, P. & Cardona, A. Fiji: an open-source platform for biological-image analysis.
905 *Nat Methods* **9,** 676–682 (2012).

906 7. Rueden, C. T., Schindelin, J., Hiner, M. C., DeZonia, B. E., Walter, A. E., Arena, E. T. &
907 Eliceiri, K. W. ImageJ2: ImageJ for the next generation of scientific image data. *BMC*
908 *Bioinformatics* **18,** 529 (2017).

909 8. Ducret, A., Quardokus, E. M. & Brun, Y. V. MicrobeJ, a tool for high throughput bacterial cell
910 detection and quantitative analysis. *Nat Microbiol* **1,** 16077 (2016).

911 9. R Core Team. *R: A language and environment for statistical computing.* (Vienna, Austria,
912 2021). at <https://www.R-project.org/>

913 10. Wickham, H., Averick, M., Bryan, J., Chang, W., McGowan, L., François, R., Grolemund, G.,
914 Hayes, A., Henry, L., Hester, J., Kuhn, M., Pedersen, T., Miller, E., Bache, S., Müller, K.,
915 Ooms, J., Robinson, D., Seidel, D., Spinu, V., Takahashi, K., Vaughan, D., Wilke, C., Woo, K.
916 & Yutani, H. Welcome to the Tidyverse. *JOSS* **4,** 1686 (2019).

917 11. Kolde, R. *Pheatmap: pretty heatmaps.* (R Package Version 1.0.10., 2019). at <https://CRAN.R-
918 project.org/package=pheatmap>

919 12. Chen, H. *VennDiagram: Generate High-Resolution Venn and Euler Plots*. (R package version
920 1.7.3, 2022). at <https://CRAN.R-project.org/package=VennDiagram>

921 13. Bolger, A. M., Lohse, M. & Usadel, B. Trimmomatic: a flexible trimmer for Illumina sequence
922 data. *Bioinformatics* **30,** 2114–2120 (2014).

923 14. Bankevich, A., Nurk, S., Antipov, D., Gurevich, A. A., Dvorkin, M., Kulikov, A. S., Lesin, V.
924 M., Nikolenko, S. I., Pham, S., Prjibelski, A. D., Pyshkin, A. V., Sirotkin, A. V., Vyahhi, N.,
925 Tesler, G., Alekseyev, M. A. & Pevzner, P. A. SPAdes: A New Genome Assembly Algorithm
926 and Its Applications to Single-Cell Sequencing. *Journal of Computational Biology* **19,** 455–477
927 (2012).

928 15. Seemann, T. Prokka: rapid prokaryotic genome annotation. *Bioinformatics* **30,** 2068–2069
929 (2014).

930 16. Li, H. Aligning sequence reads, clone sequences and assembly contigs with BWA-MEM.
931 Preprint at http://arxiv.org/abs/1303.3997 (2013)

932 17. Danecek, P., Bonfield, J. K., Liddle, J., Marshall, J., Ohan, V., Pollard, M. O., Whitwham, A.,
933 Keane, T., McCarthy, S. A., Davies, R. M. & Li, H. Twelve years of SAMtools and BCFtools.
934 *GigaScience* **10,** giab008 (2021).

935 18. Koboldt, D. C., Chen, K., Wylie, T., Larson, D. E., McLellan, M. D., Mardis, E. R., Weinstock,
936 G. M., Wilson, R. K. & Ding, L. VarScan: variant detection in massively parallel sequencing of
937 individual and pooled samples. *Bioinformatics* **25,** 2283–2285 (2009).

938 19. Cingolani, P., Platts, A., Wang, L. L., Coon, M., Nguyen, T., Wang, L., Land, S. J., Lu, X. &
939 Ruden, D. M. A program for annotating and predicting the effects of single nucleotide
940 polymorphisms, SnpEff: SNPs in the genome of *Drosophila melanogaster* strain w ^{1118} ; iso-2;
941 iso-3. *Fly* **6,** 80–92 (2012).